

Nonclassical rotational behavior at the vicinity of the λ point

Shun-ichiro Koh*

*Physics Division, Faculty of Education, Kochi University
Akebono-cho, 2-5-1, Kochi, 780, Japan*

(Dated: December 28, 2018)

The rotational property of a quantum liquid at the vicinity of the λ point T_λ is examined. In a liquid helium 4 just above T_λ , under the strong influence of Bose statistics, the coherent many-body wave function grows to an intermediate size between a macroscopic and a microscopic one, which is of a different nature from the thermal fluctuations. It must reflect in the rotational properties such as the moment of inertia. Beginning with the bosons without the condensate, we make a perturbation calculation of its susceptibility with respect to the repulsive interaction, and examine how, with decreasing temperature, the growth of the coherent wave function gradually changes the rotational behavior of a liquid: The moment of inertia slightly decreases just above T_λ . This means that at the vicinity of T_λ , the mechanical superfluid density does not always agree with the thermodynamical one. We compare the result to the experiment by Hess and Fairbank. A new interpretation of the shear viscosity just above T_λ is given from this viewpoint.

PACS numbers: 67.40.-w, 67.40.Vs, 67.40.Db, 05.30.Jp

I. INTRODUCTION

A natural way to discuss superfluidity in a confined system is to focus on its rotational properties. When a liquid helium 4 is rotated at a temperature far above the λ point T_λ , it makes a rigid-body rotation with a uniform vorticity $\text{rot}\mathbf{v} \neq 0$ owing to its viscosity. The angular momentum around z-axis has a form of $L_z^{cl} = I_z^{cl}\Omega$, where I_z^{cl} is a classical moment of inertia and Ω is a rotational velocity of a container. Figure.1 schematically shows the Ω dependence of the angular momentum. When it is cooled to a certain temperature below T_λ , it shows two different behaviors according to the value of Ω . Below the critical velocity Ω_c , it abruptly stops rotating just as the system passes the λ point, and $\text{rot}\mathbf{v} = 0$ is satisfied over the whole volume of the liquid. On the other hand, under a faster rotation than Ω_c , the uniform vorticity abruptly concentrates to certain points, forming vortex lines and leaving other areas to satisfy $\text{rot}\mathbf{v} = 0$. These phenomena instilled us with the notion that superfluidity abruptly appears at the λ point.

The basis of our phenomenological understanding is the two-fluid model, the foundation of which at $T \ll T_\lambda$ has been established by microscopic theories. The basic assumption of the two-fluid model is that it completely separates the system into the normal and superfluid part from the beginning, and assumes that the latter abruptly emerges at T_λ [1]. Furthermore, it assumes that the superfluid density defined in the mechanical properties completely agrees with that defined in thermodynamics.

Here we must make a clear definition of superfluidity. Just above T_λ , anomalies in thermodynamical or mechanical constants of a liquid, such as the λ shape of specific heat or the softening of sound propagation,

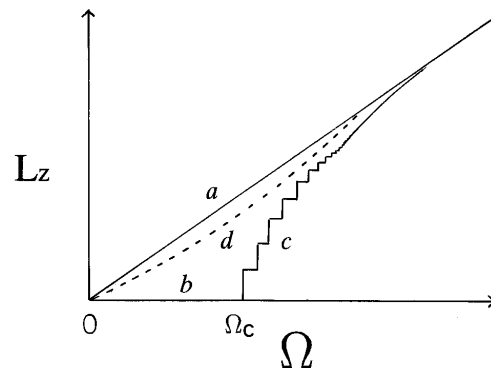


FIG. 1: The schematic Ω -dependence of the angular momentum L_z . A solid straight line a is $L_z = I_z^{cl}\Omega$ at $T \gg T_\lambda$, and a horizontal line b and a series of steps c is $L_z(\Omega)$ at $T < T_\lambda$. A dotted curve d is a subject of this paper, a size of which is exaggerated for clarity.

has been observed; These anomalies are normally considered to arise from thermal fluctuations giving rise to the short-lived randomly oriented coherent wave functions. For superfluidity, however, the long-lived collective motions of particles with a stable specific direction of motion are necessary. London stressed that superfluidity is not merely the absence of viscosity, but the occurrence of $\text{rot}\mathbf{v} = 0$, and proposed an experiment to confirm this point [2], which was later performed by Hess and Fairbank [3]. This means that the complete disappearance of shear viscosity is attributed to $\text{rot}\mathbf{v} = 0$ over the whole volume of a liquid. Hence, the thermal fluctuations, being a collection of independently growing and decaying wave functions, do not lead to superfluidity. (The relaxation time of thermal fluctuations is far shorter than the characteristic time of the macroscopic rotational exper-

*Electronic address: koh@kochi-u.ac.jp

iments. Hence, they decay long before they affect the moment of inertia.)

This paper will examine the foundation of the two-fluid model at the vicinity of the lambda point. Just above T_λ , particles experience the strong influence of Bose statistics, and therefore, the thermal-equilibrium coherent many-body wave function satisfying $\text{rot}\mathbf{v} = 0$ grows to a large but not yet macroscopic size. In contrast to thermal fluctuations, these long-lived wave functions have a possibility of affecting a mechanical property of the whole liquid, such as the moment of inertia. Specifically, they may slightly reduce the moment of inertia I_z just above T_λ , a possible $L_z(\Omega)$ of which is schematically illustrated by a dotted line d in Fig.1. This is qualitatively different from precursory phenomena owing to thermal fluctuations in that it requires a stable specific direction of motion. If it is true, it allows us to redefine the superfluid density in the mechanical phenomena. This means that at the vicinity of T_λ , the mechanical superfluid density does not always agree with the thermodynamical superfluid density.

The rotational properties of a liquid helium 4 has been subjected to considerable experimental and theoretical studies [4]. These studies, however, mainly focus on the dynamics of the quantized vortices in the superfluid phase in situations where the rotational velocity is not so small that the number of vortices are large. After the pioneering work by Hess and Fairbank [3], and by Packard and Sanders [5], the regimes in which only a few vortices are present have rarely been explored. Hence, it is not surprising that almost no precise measurement has been made on I_z just above the λ point.

A similar reason exists in theoretical studies as well. In theories of superfluidity, the infinite-volume limit is often assumed. In $V \rightarrow \infty$, the only significant distinction between states is that between the microscopic and macroscopic one, and therefore there is no room for the intermediate-sized wave functions in the theory. (In $V \rightarrow \infty$, “large but not yet macroscopic” is substantially equivalent to “microscopic” [6].) This clear-cut distinction lies behind the two-fluid model, and leads us to the preoccupied notion that superfluidity appear in a mathematically discontinuous manner at the Bose-Einstein condensation temperature T_{BEC} . For the real system, however, the overall transformation occurs more or less continuously. For the rotation of confined system, one cannot ignore the existence of the center of rotation and the boundary of the system, and therefore, one must take into account the size of the system. Hence, the validity of the limit $V \rightarrow \infty$ is worth examination, and the magnitude of phenomena hidden in the $V \rightarrow \infty$ limit must be estimated by experiments.

(1) When one views previous experiments of a liquid helium 4 from this point, one notes in the data by Hess and Fairbank an experimental sign suggesting a slight decrease of I_z just above T_λ (see Sec.4A).

(2) The trapped atomic Bose gas opens a new possibility of precise measurements of I_z just above T_c . The

measurement of the angular momentum using the precession of a Bose-Einstein condensate of ^{87}Rb atoms was performed [7], which is analogous to the experiment by Hess and Fairbank, and by Packard and Sanders in a bulk liquid helium 4. It gives a data of $L_z(\Omega)$ like b and c in Fig.1 (Fig.2 of Ref.[7]). Since the trapped Bose gas is a small system ($\cong 4\mu\text{m}$), its Ω_c is 10^4 times larger than that of a liquid helium 4 in Ref. [3] and [5], which enables us to realize a situation in which only a few vortices are present. Whereas studies in this field are now centered on the anomalous behaviors at $T \ll T_c$, it has the potential for showing a slight change of I_z just above T_c .

Although the deviation of the moment of inertia I_z just above T_λ from its classical value may be small, the essence of superfluidity is revealed in a primitive form in such a regime, which constitutes the necessary condition for discriminating a quantum fluid from a classical fluid. To consider these problems, we will make a somewhat different approach from conventional ones. At $T < T_\lambda$, the existence of the macroscopic coherent wave function $\phi(\mathbf{r}) = |\phi| \exp[iS(\mathbf{r})]$ (\mathbf{r} is a center-of-mass coordinate of many helium 4 atoms) leads to $\text{rot}\mathbf{v} = 0$ geometrically, because the condensate momentum \mathbf{p} is expressed by $\mathbf{p} = (\hbar/m)\nabla S$. Since we will focus on the continuous change of the system around T_λ , we cannot assume from the beginning the sudden emergence of $\phi(\mathbf{r})$ at T_λ . Rather, considering the Bose system above and below T_λ on a common ground will enable us to study the intricacy underlying the onset of superfluidity. We begin with the Bose system *without the condensate*, make a perturbation calculation of its susceptibility with respect to the repulsive interaction by taking peculiar graphs reflecting Bose statistics, and examine how the formation of the coherent wave function gradually changes the rotational behavior of the system. As a result, we derive a nonclassical rotational behavior that we normally think comes from $\text{rot}\mathbf{v} = 0$, *without assuming* $\text{rot}\mathbf{v} = 0$ *from the beginning*. Specifically, we will derive the decrease of I_z like d in Fig.1 in the rotating repulsive Bose system just above T_λ , and compare it with the data in a liquid helium 4.

This paper is organized as follows. Section 2 recapitulates the definition of the moment of inertia, and explains the physical reason of the nonclassical rotational behavior. Section 3 develops a formalism of the linear response of the system. (For the difference between this formalism and the thermal fluctuation theories, see Appendix.A.) Using the result in Sec.3, Sec.4 re-examines the experiment by Hess and Fairbank, and estimates the size of the intermediate-sized wave function and the strength of repulsive interaction in a liquid helium 4. Section 5 considers the nonlinear response. From this viewpoint, Sec.6 gives a new interpretation of the observed decrease of shear viscosity just above T_λ in a liquid helium 4, and discusses some other examples.

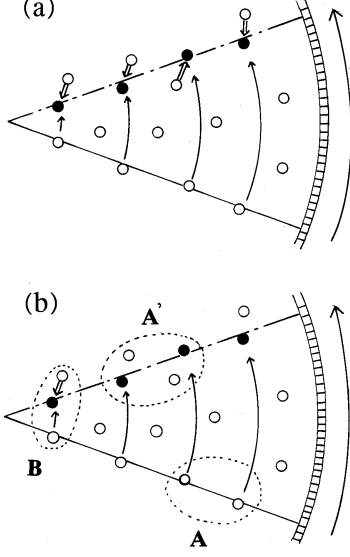


FIG. 2: Schematic pictures of a part of the rotating bosons in a cylindrical container. White circles represent a initial distribution of particles. The rotation by long arrows moves white circles on a solid-line radius to black circles. (a) At $T < T_\lambda$, the permutation symmetry holds over the whole liquid. (b) Just above T_λ , it holds only within limited areas enclosed by a dotted lines, a size of which is exaggerated for clarity.

II. MOMENT OF INERTIA OF THE REPULSIVE BOSE SYSTEM

A. Moment of inertia

Consider bosons in a uniform rotation around z-axis. For a liquid helium 4, the repulsive particle picture is not so unrealistic as it would be for any other liquid. Hence, as its simplest model, we use

$$H = \sum_p \epsilon(p) \Phi_p^\dagger \Phi_p + U \sum_{p,p'} \sum_q \Phi_{p-q}^\dagger \Phi_{p'+q}^\dagger \Phi_{p'} \Phi_p, \quad (U > 0), \quad (1)$$

where Φ_p denotes an annihilation operator of a spinless boson.

The hamiltonian in a coordinate system rotating with a container is $H - \mathbf{\Omega} \cdot \mathbf{L}$, where \mathbf{L} is the total angular momentum. The rotation is equivalent to the application of a probe acting on a sample [8] [9]. The perturbation $H_{ex} = -\mathbf{\Omega} \cdot \mathbf{L}$ is cast in the form $-\sum_i (\mathbf{\Omega} \times \mathbf{r}) \cdot \mathbf{p}$, in which $\mathbf{\Omega} \times \mathbf{r} \equiv \mathbf{v}_d(\mathbf{r})$ serves as the external field. Figure.2 shows a part of the Bose system in a cylindrical container. When the origin of \mathbf{r} is put on the center of rotation, $\mathbf{v}_d(\mathbf{r})$ has a concentric-circle structure illustrated by curved arrows in Fig.2. (In the rigid-body rotation, $\mathbf{v}_d(\mathbf{r})$ agrees with the drift velocity at point \mathbf{r} .) We define a mass-current density $\mathbf{J}(\mathbf{r})$, and express the

perturbation H_{ex} as

$$-\mathbf{\Omega} \cdot \mathbf{L} = - \int \mathbf{v}_d(\mathbf{r}) \cdot \mathbf{J}(\mathbf{r}) d^3x. \quad (2)$$

Because of $\text{div} \mathbf{v}_d(\mathbf{r}) = 0$, Eq.(2) says that $\mathbf{v}_d(\mathbf{r})$ acts as a transverse-vector probe to the excitation of bosons. This fact allows us the formal analogy that the response of the system to $\mathbf{v}_d(\mathbf{r})$ is analogous to the response of the charged Bose system to the vector potential $\mathbf{A}(\mathbf{r})$ in the Coulomb gauge. Hence, $\mathbf{J}(\mathbf{r})$ in Eq.(2) has the following form in momentum space being similar to that in the charged Bose system

$$J_\mu(q, \tau) = \sum_{p,n} \left(p + \frac{q}{2} \right)_\mu \Phi_p^\dagger \Phi_{p+q} e^{-i\omega_n \tau}, \quad (3)$$

($\hbar = 1$ and $\tau = it$). $\mathbf{v}_d(\mathbf{r})$ is a macroscopic external field causing the spatial inhomogeneity in the container, whereas $\mathbf{J}(\mathbf{r})$ contains both microscopic and macroscopic informations of the system.

As the simplest susceptibility to $\mathbf{v}_d(\mathbf{r})$, we often use the mass density $\rho = nm$ (n is the number density of particles) as $\mathbf{J}(\mathbf{r}) = \rho \mathbf{v}_d(\mathbf{r})$. Microscopically, however, one must begin with the generalized susceptibility consisting of the longitudinal and transverse part ($\mu = x, y, z$)

$$\chi_{\mu\nu}(q, \omega) = \frac{q_\mu q_\nu}{q^2} \chi^L(q, \omega) + \left(\delta_{\mu\nu} - \frac{q_\mu q_\nu}{q^2} \right) \chi^T(q, \omega). \quad (4)$$

By definition, the mass density ρ is a longitudinal response to an external force, $\rho = \chi^L(0, 0)$. As illustrated in Fig.2, however, the rotational motion of particles is perpendicular to the radial direction, along which the influence of the wall motion extends into the container. Hence, in principle, one must use the transverse susceptibility $\chi^T(q, \omega)$ for $\mathbf{v}_d(\mathbf{r})$ such as $\mathbf{J}(\mathbf{r}) = [\lim_{q \rightarrow 0} \chi^T(q, 0)] \mathbf{v}_d(\mathbf{r})$.

Using $\mathbf{\Omega} = (0, 0, \Omega)$ in the left-hand side of Eq.(2) and the above $\mathbf{J}(\mathbf{r})$ and $\mathbf{v}_d = \mathbf{\Omega} \times \mathbf{r} = (-\Omega y, \Omega x, 0)$ in its right-hand side, one obtains the angular momentum L_z as

$$L_z = \chi^T(0, 0) \int_V (x^2 + y^2) d^3x \cdot \Omega. \quad (5)$$

In a normal fluid, the susceptibility satisfies $\chi^T(0, 0) = \chi^L(0, 0)$, and therefore the ordinary use of ρ is justified. The classical moment of inertia is given by

$$I_z^{cl} = mn \int_V (x^2 + y^2) d^3x = \chi^L(0, 0) \int_V (x^2 + y^2) d^3x. \quad (6)$$

In a superfluid, however, the above argument must be altered. For the later use, we define a term proportional to $q_\mu q_\nu$ in $\chi_{\mu\nu}$ by $\hat{\chi}_{\mu\nu}$

$$\begin{aligned} \chi_{\mu\nu}(q, \omega) &= \delta_{\mu\nu} \chi^T(q, \omega) + q_\mu q_\nu \left(\frac{\chi^L(q, \omega) - \chi^T(q, \omega)}{q^2} \right) \\ &\equiv \delta_{\mu\nu} \chi^T(q, \omega) + \hat{\chi}_{\mu\nu}(q, \omega), \end{aligned} \quad (7)$$

where $\hat{\chi}_{\mu\nu}$ represents the balance between the longitudinal and transverse susceptibility [10]. Comparing Eq.(5) to Eq.(6), one writes the moment of inertia $I_z = L_z/\Omega$ using $\hat{\chi}_{\mu\nu}$

$$I_z = I_z^{cl} \left(1 - \frac{1}{\rho} \lim_{q \rightarrow 0} \left[\frac{q^2}{q_\mu q_\nu} \hat{\chi}_{\mu\nu}(q, 0) \right] \right). \quad (8)$$

For the occurrence of nonclassical moment of inertia, the balance between the longitudinal and transverse low-energy excitation must be destroyed. In Eq.(8), $\lim_{q \rightarrow 0} [(q^2/q_\mu q_\nu) \hat{\chi}_{\mu\nu}(q, 0)]$ corresponds to the superfluid density ρ_s .

Consider $\chi_{\mu\nu}$ of the ideal Bose system. Within the linear response, it is defined as

$$\chi_{\mu\nu}^{(1)}(q, \omega_n) = \frac{1}{V} \int_0^\beta d\tau \exp(i\omega_n \tau) \langle 0 | T_\tau J_\mu(q, \tau) J_\nu(q, 0) | 0 \rangle, \quad (9)$$

where $|0\rangle$ is the ground state of $\sum_p \epsilon(p) \Phi_p^\dagger \Phi_p$. The term proportional to $q_\mu q_\nu$ has a form of

$$\hat{\chi}_{\mu\nu}^{(1)}(q, \omega) = -\frac{q_\mu q_\nu}{4} \frac{1}{V} \sum_p \frac{f(\epsilon(p)) - f(\epsilon(p+q))}{\omega + \epsilon(p) - \epsilon(p+q)}, \quad (10)$$

where $f(\epsilon(p))$ is the Bose distribution.

(1) If bosons would form the condensate, $f(\epsilon(p))$ in Eq.(10) is a macroscopic number for $p = 0$ and nearly zero for $p \neq 0$. Thus, in the sum over p in the right-hand side of Eq.(10), only two terms corresponding to $p = 0$ and $p = -q$ remain, with a result that

$$\hat{\chi}_{\mu\nu}^{(1)}(q, 0) = \rho_s(T) \frac{q_\mu q_\nu}{q^2}, \quad (11)$$

where $\rho_s(T) = mn_c(T)$ is the thermodynamical superfluid density, and $n_c(T)$ is the number density of particles participating in the condensate. Equation.(8) with Eq.(11) leads to

$$I_z = I_z^{cl} \left(1 - \frac{\rho_s(T)}{\rho} \right). \quad (12)$$

(2) When bosons form no condensate, the sum over p in Eq.(10) is carried out by replacing it with an integral, and one notes that q^{-2} dependence disappears in the result. Hence, using such a $\hat{\chi}_{\mu\nu}^{(1)}(q, \omega)$ in Eq.(8) leads to $I_z = I_z^{cl}$ at $q \rightarrow 0$. This means that, without the interaction between particles, BEC is the necessary condition for the nonclassical moment of inertia.

Under the repulsive interaction, however, the above argument is seriously affected. To see this, we must begin with a physical argument.

B. Bose statistics and repulsive interaction

We have a physical reason to expect the decrease of the moment of inertia in bosons at low temperature.

The relationship between the low-energy excitations and Bose statistics dates back to Feynman's argument on the scarcity of the excitation in a liquid helium 4 [11], in which he explained how Bose statistics affects the many-body wave function in configuration space. To the rotating bosons, we will apply his explanation.

(1) In Fig.2(a), a liquid (white circles) is in the BEC phase, and the wave function has permutation symmetry everywhere in the container. Assume that the rotation of a container (depicted by curved arrows) moves white circles on a solid-line radius to black circles on a one-point-dotted-line radius (a transverse excitation). At first sight, these displacements seem to be a large-scale configuration change, but this result is reproduced by a set of slight displacements (depicted by short thick arrows) from positions in the initial configuration to black circles after rotation. For any particle after rotation, it is possible to find a particle being close to it in the initial configuration. In Bose statistics, owing to permutation symmetry, one cannot distinguish between two types of particles after rotation, one moved from the neighboring position by the short arrow, and the other moved from distant initial positions by the long arrow. Even if the displacement made by the long arrows is a large displacement in classical statistics, it is only a slight displacement by the short arrows in Bose statistics.

Let us imagine this situation in the 3N-dimensional configuration space. The above feature of Bose statistics means that in the configuration space, the excited state driven by rotation lies close to the ground state. Since the excited state is orthogonal to the ground state, the wave function corresponding to the excited state must spatially oscillate. Accordingly, the many-body wave function of the transversely excited state oscillates within a small distance in configuration space. Since the kinetic energy of the system is determined by the 3N-dimensional gradient of the wave function, this steep rise and fall of the amplitude means that the energy of the transverse excitation is not small even at $q = 0$, leading to the scarcity of the low-energy transverse excitation. This is the reason of $\chi^T(q, 0) \rightarrow 0$ at $q \rightarrow 0$ below T_λ , whereas the particle conservation asserts that $\chi^L(q, 0) = \rho$ is valid both above and below T_λ . Hence, $\hat{\chi}_{\mu\nu}(q, 0)$ in Eq.(7) changes to $\rho q_\mu q_\nu / q^2$ at $q \rightarrow 0$, leading to $I_z = 0$ in Eq.(8). (This mechanism underlies the geometrical condition $rot \mathbf{v}_s = 0$.)

(2) At high temperature, the coherent wave function has a microscopic size. If a long arrow of $\mathbf{v}_d(\mathbf{r})$ takes a particle to a position beyond the coherent wave function including that particle, one cannot regard the particle after rotation as an equivalent of the initial one. The mechanism below T_λ does not work for the large displacement extending over two different wave functions. Hence, we obtain $\chi^T(q, 0) = \chi^L(q, 0)$ at $q \rightarrow 0$, and $I_z = I_z^{cl}$.

(3) Figure.2(b) shows the boson system at the vicinity of T_λ in the normal phase, in which the coherent many-body wave function grows to a large but not yet a macroscopic size (regions enclosed by a dotted line).

The permutation symmetry holds only within each of these regions. When particles are moved from a region A to another region A', the mechanism below T_λ does not work.

The repulsive interaction U between particles, however, affects this situation. In general, when one moves a particle in the interacting system, it induces the motions of other particles. In particular, the large-distance displacement of a particle in coordinate space causes the excitation of many particles, and therefore it needs a large excitation energy. This means, in the low-energy excitation of the system, one observes mainly the short-distance displacement of particles. When applying this tendency to the low-energy excitation of repulsive bosons, one knows that *excited particles are not likely to go beyond a single coherent wave function, but likely to remain in it, and therefore the mechanism working below T_λ works just above T_λ as well.* This view will be tested as follows. If we increase the strength of U in $\chi_{\mu\nu}(q, 0)$, the excited bosons get to remain in the same coherent wave function, and therefore the low-energy transverse excitation will raise its energy owing to Bose statistics as discussed in (1). Hence, the condition of $\chi^L(q, 0) = \chi^T(q, 0)$ at $q \rightarrow 0$ will be violated at a certain critical value of U . Alternatively, *if we decrease the temperature at a given U , the above condition will be violated at a certain temperature T_{on} .*

A geometric feature inherent in the rotation will play an important role in the above mechanism. The external field $\mathbf{v}_d(\mathbf{r})$ has the structure of concentric circle; hence, the center of rotation is a fixed point. The displacements of particles near the center is so small that they do not go beyond a single coherent wave function (a region B in Fig.2(b)). The center of rotation is the most probable point for the mechanism discussed in (a) to work. Hence, the region near the center is most likely to decouple from the motion of container. With decreasing temperature, this decoupling will extend from the center to the wall, which depends on the rotational velocity Ω .

To formulate these mechanisms, we consider the perturbation expansion of $\chi_{\mu\nu}$ with respect to U in Sec.3. After comparing it with the experiment in Sec.4, we extend it to the nonlinear response to $\mathbf{v}_d(\mathbf{r})$ in Sec.5.

III. LINEAR RESPONSE

We will formulate the moment of inertia in the repulsive Bose system at the vicinity of T_λ . In the integrand of Eq.(9), one must use, instead of $|0\rangle$, the ground state $|G\rangle$ of Eq.(1) as follows

$$\begin{aligned} & \langle G | T_\tau J_\mu(x, \tau) J_\nu(0, 0) | G \rangle \\ &= \frac{\langle 0 | T_\tau \hat{J}_\mu(x, \tau) \hat{J}_\nu(0, 0) \exp \left[- \int_0^\beta d\tau \hat{H}_I(\tau) \right] | 0 \rangle}{\langle 0 | \exp \left[- \int_0^\beta d\tau \hat{H}_I(\tau) \right] | 0 \rangle} \quad (13) \end{aligned}$$

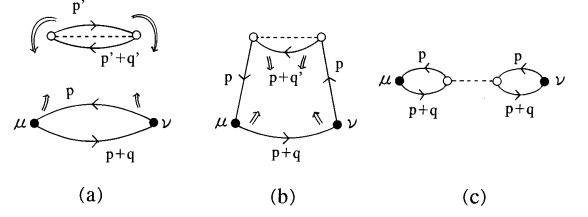


FIG. 3: (a) The first-order Feynman diagram of a current-current response tensor $J_\mu J_\nu$ (a lower bubble), and an excitation owing to the repulsive interaction U (an upper bubble with a dotted line). The black and white small circle represents a vector and scalar vertex, respectively. The exchange of particle lines between the excitation and the response tensor yields (b). Similarly, the interchange of particle lines in a deformed square yields (c).

where $\hat{H}_I(\tau)$ represents the repulsive interaction. Figure 3(a) illustrates the current-current response tensor $\hat{J}_\mu(x, \tau) \hat{J}_\nu(0, 0)$ in the medium: Owing to $\exp(-\int \hat{H}_I(\tau) d\tau)$ in Eq.(13), scatterings of particles frequently occur in $|G\rangle$ as illustrated by an upper bubble with a dotted line U in Fig.3(a). (The black and white circle represents a coupling to $\mathbf{v}_d(\mathbf{q})$ and to U , respectively.) The state $|G\rangle$ includes many interaction bubbles like the upper one in Fig.3(a) with various momentums p' and $p'+q'$. A solid line with an arrow represents

$$G(i\omega_n, p) = \frac{1}{i\omega_n - \epsilon(p) - \Sigma + \mu}. \quad (14)$$

(μ is a chemical potential implicitly determined by $V^{-1} \Sigma [\exp(\beta[\epsilon(q) + \Sigma - \mu]) - 1]^{-1} = n$). Owing to the repulsive interaction, the boson has a self energy Σ (> 0) (we ignore its ω and p dependence by assuming it small). With decreasing temperature, the negative μ at high temperature approaches a small positive value of Σ , finally reaching Bose-Einstein condensation satisfying $\mu = \Sigma$.

When the system is just above T_λ in the normal phase, particles in the ground state $|G\rangle$ are under the strong influence of Bose statistics. Hence, the perturbation must be developed in such a way that, as the order of the perturbation increases, the susceptibility gradually includes a new effect owing to Bose statistics. Specifically, the lower bubble $\hat{J}_\mu(x, \tau) \hat{J}_\nu(0, 0)$ and the upper bubble in Fig.3(a) form a coherent wave function as a whole. When one of the two particles in both the lower and upper bubble have the same momentum ($p = p'$), and the other in both bubbles have another same momentum ($p+q = p'+q'$) in Fig.3(a), a graph made by exchanging these particles must be included in the expansion. Such a transformation in Fig.3(a) takes place as follows. The exchange of two particles having p and $p' (= p)$ by thick white arrows yields Fig.3(b). Furthermore, the interchange of two particles having $p+q$ and $p+q' (= p+q)$ in Fig.3(b) by thick white arrows yields Fig.3(c). The result is that two bubbles with the same momentum are

linked by the repulsive interaction, the contribution of which to $\chi_{\mu\nu}$ is given by

$$U \frac{1}{V} \sum_p \left(p + \frac{q}{2}\right)_\mu \left(p + \frac{q}{2}\right)_\nu \times \left[-\frac{f(\epsilon(p) + \Sigma) - f(\epsilon(p + q) + \Sigma)}{\omega + \epsilon(p) - \epsilon(p + q)} \right]^2. \quad (15)$$

(a) With decreasing temperature, the coherent wave function grows to a large size, and the interchange of particles owing to Bose statistics like Fig.3 occurs many times. Hence, one cannot ignore the higher-order terms in Eq.(13), which become more significant with the growth of the coherent wave function.

(b) Among many particles contributing to Eq.(15), particles stationary to a container play a dominant role. Specifically, a term with $p = 0$ in Eq.(15) corresponds to an excitation from the rest particle, and that with $p = -q$ corresponds to a decay into the rest one.

These two considerations (a) and (b) lead to the following form of $\hat{\chi}_{\mu\nu}^{(1)}(q, 0)$ at the vicinity of T_λ

$$\hat{\chi}_{\mu\nu}^{(1)}(q, 0) = \frac{q_\mu q_\nu}{2} \frac{1}{V} \sum_{l=0}^{\infty} U^l F_\beta(q)^{l+1}, \quad (16)$$

where $F_\beta(q)$ is

$$\frac{(\exp(\beta[\Sigma - \mu]) - 1)^{-1} - (\exp(\beta[\epsilon(q) + \Sigma - \mu]) - 1)^{-1}}{\epsilon(q)}, \quad (17)$$

a positive monotonously decreasing function of q^2 , which approaches zero as $q^2 \rightarrow \infty$.

At a high temperature ($\beta\mu \ll 0$) in which $F_\beta(q)$ is small, a small $F_\beta(q)$ guarantees the convergence of an infinite series in $\hat{\chi}_{\mu\nu}^{(1)}(q, 0)$ of Eq.(16), with a result that

$$\hat{\chi}_{\mu\nu}^{(1)}(q, 0) = \frac{q_\mu q_\nu}{2} \frac{1}{V} \frac{F_\beta(q)}{1 - UF_\beta(q)}. \quad (18)$$

With decreasing temperature, however, the negative μ gradually approaches Σ , hence $\Sigma - \mu \rightarrow 0$. Since $F_\beta(q)$ increases as $\Sigma - \mu \rightarrow 0$, it makes the higher-order term significant in Eq.(16). An expansion form of $F_\beta(q) = F_\beta(0) - aq^2 + \dots$ around $q^2 = 0$ has a form such as

$$F_\beta(q) = \frac{\beta}{4 \sinh^2 \left(\frac{|\beta[\mu(T) - \Sigma]|}{2} \right)} \times \left[1 - \frac{\beta}{2} \frac{1}{\tanh \left(\frac{|\beta[\mu(T) - \Sigma]|}{2} \right)} \frac{q^2}{2m} + \dots \right]. \quad (19)$$

At $q \rightarrow 0$, the denominator $1 - UF_\beta(q)$ in the right-hand side of Eq.(18) has a form of $[1 - UF_\beta(0)] + Uaq^2$.

In $\Sigma - \mu \rightarrow 0$, $UF_\beta(0)$ increases and finally reaches 1, that is,

$$U\beta = 4 \sinh^2 \left(\frac{\beta[\mu(T) - \Sigma(U)]}{2} \right). \quad (20)$$

At this point, the denominator in the right-hand side of Eq.(18) gets to begin with q^2 , and $\hat{\chi}_{\mu\nu}^{(1)}(q, 0)$ therefore changes to a form of $q_\mu q_\nu / q^2$ at $q \rightarrow 0$. This means that a non-zero coefficient $F_\beta(0)/(2VUa)$ of $q_\mu q_\nu / q^2$ appearing in Eq.(18) gives a non-zero value of $\chi^L(q, 0) - \chi^T(q, 0)$ in Eq.(7), hence the moment of inertia shows the nonclassical behavior in Eq.(8).

From now, we call T satisfying Eq.(20) *the onset temperature of the nonclassical moment of inertia* T_{on} [12].

At the vicinity of T_λ , Eq.(20) is approximated as $U\beta = \beta^2[\mu(T) - \Sigma(U)]^2$ for a small $\mu - \Sigma$. This condition has two solutions $\mu(T) = \Sigma(U) \pm \sqrt{Uk_B T}$. It is generally assumed that the repulsive Bose system undergoes BEC as well as a free Bose gas. Hence, with decreasing temperature, $\mu(T)$ in the presence of repulsive interaction U should reach $\Sigma(U)$ at a finite temperature, during which course the system necessarily passes a state satisfying $\mu(T) = \Sigma(U) - \sqrt{Uk_B T}$ [13]. One concludes that *the nonclassical rotational behavior always occurs prior to BEC in the repulsive bosons*, that is, $T_{on} > T_\lambda$.

The chemical potential μ , hence $\mu - \Sigma$ as well, determines the size of the coherent many-body wave function [14][15], which corresponds to the size of regions enclosed by a dotted line in Fig.2(b). *The emergence of q^{-2} singularity in $\hat{\chi}_{\mu\nu}^{(1)}(q, 0)$ in the process of $\Sigma - \mu \rightarrow 0$ is a mathematical expression of the instability mechanism induced by the growth of the coherent wave function.* When U is small, this instability occurs after the wave function grows to a large size corresponding to a small $\Sigma - \mu$. When U is large, this instability already occurs at a larger $\Sigma - \mu$ in which the wave function is smaller than the former one.

At the onset temperature T_{on} , substituting Eq.(19) into Eq.(18), we find $\hat{\chi}_{\mu\nu}^{(1)}$ at $q \rightarrow 0$

$$\hat{\chi}_{\mu\nu}^{(1)}(q, 0) = \frac{2m}{U\beta_{on}} \frac{1}{V} \tanh \left(\frac{|\beta_{on}[\mu(T_{on}) - \Sigma]|}{2} \right) \frac{q_\mu q_\nu}{q^2}, \quad (21)$$

and with the aid of Eq.(20)

$$\hat{\chi}_{\mu\nu}^{(1)}(q, 0) = \frac{1}{V} \frac{m}{\sinh |\beta_{on}[\mu(T_{on}) - \Sigma]|} \frac{q_\mu q_\nu}{q^2}. \quad (22)$$

$\hat{\chi}_{\mu\nu}^{(1)}(q, 0)$ is given by

$$\hat{\chi}_{\mu\nu}^{(1)}(q, 0) = mc(T_{on})n_0(T_{on}) \frac{q_\mu q_\nu}{q^2}, \quad (23)$$

where

$$n_0(T) = \frac{1}{V} \frac{1}{\exp(-\beta[\mu(T) - \Sigma]) - 1}, \quad (24)$$

is the number density of $p = 0$ bosons, and

$$c(T) = \frac{2}{\exp(\beta|\mu(T) - \Sigma|) + 1}, \quad (25)$$

is a Fermi-distribution-like coefficient. For the finite system just above T_λ , $n_0(T)$ has a large but not yet macroscopic value. In the theoretical limit $V \rightarrow \infty$, this quantity is normally regarded to be zero. In real finite system, however, its magnitude must be estimated by experiments (see Sec.4). Using Eq.(23) in Eq.(8), we obtain

$$I_z(T_{on}) = I_z^{cl} \left(1 - c(T_{on}) \frac{n_0(T_{on})}{n} \right) \equiv I_z^{cl} \left(1 - \frac{\hat{\rho}_s(T_{on})}{\rho} \right). \quad (26)$$

where $\hat{\rho}_s(T) \equiv mc(T)n_0(T)$ is the *mechanical superfluid density*.

$\hat{\rho}_s(T)$ reflects the intermediate-sized coherent wave function. “Intermediate” means that it does not play the role of order parameter characterizing the thermodynamical phase, but affects mechanical properties of the system. At $T = T_{on}$, the system shows a small but finite jump from I_z^{cl} to I_z , which is proportional to $n_0(T_{on})$. Since $c(T_{on})$ has an order of one, the magnitude of this jump is determined mainly by the non-macroscopic $n_0(T_{on})$ and the moment of inertia therefore only slightly decreases from the classical value. (This does not mean that the thermodynamical quantities show a finite jump.) At $T < T_{on}$, the moment of inertia varies with T following $I_z(T)$ in Eq.(26). Equation (26) determines an initial slope of the dotted curve d at $\Omega = 0$ in Fig.1. When the system reaches $T = T_\lambda$, the condition of $\mu = \Sigma$ makes $\hat{\rho}_s(T_\lambda) = \rho_s(T_\lambda)$ because of $c(T_\lambda) = 1$, $n_0(T_\lambda) = n_c$, which shows a natural connection of Eq.(26) to Eq.(12) with the thermodynamical $\rho_s(T)$. While the thermodynamical $\rho_s(T)$ satisfy $\rho_s = (m^2 k_B T / \hbar^2) |\phi|^2$ at $T < T_\lambda$, one can expect no simple relation of the mechanical $\hat{\rho}_s(T)$ with the thermodynamical quantities at $T_\lambda < T < T_{on}$.

IV. COMPARISON TO EXPERIMENTS

A. Experiment by Hess and Fairbank revisited

Hess and Fairbank, after they confirmed that a superfluid 4 below T_λ remained at rest under the extremely slow rotation, made another type of experiment in their classic paper Ref.[3]. First, at an initial temperature T_1 below or above T_λ , they rotated a liquid helium 4, contained in a small cylinder of radius $R = 0.44$ mm, at $\Omega = 1.13$ rad/s. Later they heated it up to the temperature as it comes into rigid-body rotation, and precisely measured a small change $\Delta\Omega$ of the angular velocity. Using Eq.(12), the rotational energy before heating is $1/2 \times I_z^{cl} (1 - \rho_s/\rho) \Omega^2$, whereas it changes to $1/2 \times I_z^{cl} (\Omega - \Delta\Omega)^2$ after heating. By the conservation of energy, the former must be equal to the latter, with a result that $2\Delta\Omega/\Omega \cong \rho_s/\rho$. Below T_λ , a fraction of

liquid does not participate in the rotation, whereas after heating it does. The rotation after heating therefore always becomes slower, and $2\Delta\Omega/\Omega \cong \rho_s/\rho$ is positive. They plotted $\Delta\Omega/\Omega$ as a function of initial temperature T_1 (Fig.2 of Ref.[3]).

When the initial temperature T_1 was lower than T_λ , $\Delta\Omega/\Omega$ was properly explained by the theoretical value of $\rho_s(T_1)/\rho$. If the two-fluid model is exactly valid near T_λ , ρ_s must vanish at $T > T_\lambda$. Hence, $\Delta\Omega/\Omega$ measured under the condition of $T_1 > T_\lambda$ must be exactly zero. For $T_1 = T_\lambda + 0.03K$ and $T_\lambda + 0.28K$, however, the measured $\Delta\Omega/\Omega$ in Ref [3] were not exactly zero. Although the error bars were large compared with its absolute values, its central values were significantly different from zero: $\Delta\Omega/\Omega \cong 4 \times 10^{-5}$ at $T_1 = T_\lambda + 0.03K$, and 1.5×10^{-5} at $T_\lambda + 0.28K$. A natural interpretation of this result is that these T_1 's were lower than the onset temperature T_{on} of the nonclassical moment of inertia, and at such T_1 's, I_z was already slightly smaller than its classical value. If it is true, instead of Eq.(12), $I_z(T) = I_z^{cl} (1 - \hat{\rho}_s(T)/\rho)$ (Eq.(26)) must be used, and we obtain $2\Delta\Omega/\Omega \cong \hat{\rho}_s(T_1)/\rho$. Hence, we obtain $\hat{\rho}_s(T_\lambda + 0.03K)/\rho \cong 8 \times 10^{-5}$, and $\hat{\rho}_s(T_\lambda + 0.28K)/\rho \cong 3 \times 10^{-5}$ [16]. Since the number density of atoms in a liquid helium 4 is $n \cong 2.2 \times 10^{22}$ atoms/cm³, we have $n_0 \cong 10^{18}$ atoms/cm³. This is an experimental estimation of the number of helium 4 atoms participating in the intermediate-sized coherent wave function in a bulk helium 4 just above T_λ . Two temperatures, $T_\lambda + 0.03K$ and $T_\lambda + 0.28K$, are situated within the temperature region ($T_\lambda < T < 2.8$ K) in which the viscosity begins to decrease above T_λ . In Ref.[3], the author's focus was on the rigidity of a superfluid against the rotation (the result was later named Hess-Fairbank effect), and they did not mention the small non-zero value of $\Delta\Omega/\Omega$ above T_λ . Although this point did not attract the interest of many people, it is worth studying closely in the future.

B. Estimation of the repulsive interaction U

Let us make an estimation of the repulsive interaction U using the approximate form of Eq.(20), $U\beta_{on} = \beta_{on}^2 (\mu - \Sigma)^2$. (1) For the present, we suppose $T_{on} = 2.8K$ by assuming that the decrease of viscosity just above T_λ has a relation to the emergence of the intermediate-sized coherent wave function (see Sec.6.A). (2) We assume that $\mu(T) - \Sigma(U)$ in Eq.(20) follows the formula

$$\mu(T) - \Sigma(U) = - \left(\frac{g_{3/2}(1)}{2\sqrt{\pi}} \right)^2 k_B T_\lambda \left[\left(\frac{T}{T_\lambda} \right)^{3/2} - 1 \right]^2, \quad (27)$$

($g_a(x) = \sum_n x^n / n^a$) on the assumption that the particle interaction U and the particle density of a liquid helium 4 are renormalized to $T_\lambda = 2.17K$ (an approximation that dates back to London). Hence, we obtain a rough estimation of U as 0.5×10^{-17} erg. This value is approximately close to the repulsive interaction U_c obtained by

Bogoliubov's spectrum $c = (\hbar/m)\sqrt{4\pi na}$, but somewhat smaller than it. (The velocity of ordinary sound $c = 220$ m/s of a liquid helium 4 near T_λ gives a scattering length $a = 0.7$ nm, hence $U_c \cong \hbar^2/(ma^2) = 3.4 \times 10^{-17}$ erg.) It is a difficult problem to relate these values to the realistic potential between helium 4 atoms such as the Lennard-Jones potential $U(r) = 4\epsilon[(2.556/r)^{12} - (2.556/r)^6]$ with $\epsilon = 1.41 \times 10^{-15}$ erg.

V. NONLINEAR RESPONSE

When the precise measurement of I_z is performed, the dynamic response of $I_z(\Omega)$ will become a next subject, which appears in the nonlinear response of the system. As discussed in Sec.2, \mathbf{J} contains both microscopic and macroscopic information, whereas $\mathbf{v}_d(\mathbf{r})$ is a macroscopic external field, and therefore the susceptibility connecting \mathbf{J} and \mathbf{v}_d appears as $\mathbf{J}(\mathbf{r}) = [\lim_{q \rightarrow 0} \chi^T(q, 0)] \mathbf{v}_d(\mathbf{r})$. Hence, we consider not a general form of the nonlinear susceptibility, but a correction term $\chi^{T, non}(v_d)$ to the linear response, such as $\mathbf{J} = [\chi^{T, (1)} + \chi^{T, non}(v_d)] \mathbf{v}_d$. Since $\chi^{T, non}(v_d)$ does not depend on the direction of \mathbf{v}_d , it includes only even powers of $v_d = \Omega r$, which leads to the spatial inhomogeneity and the dynamic response.

For the dynamic response, we define some quantities. The current $\mathbf{J}(\mathbf{r}) = \chi^T(0, 0) \mathbf{v}_d(\mathbf{r})$ in Sec.2.A is replaced by $\mathbf{J}(\mathbf{r}) = \chi^T(0, 0, \Omega, r) \mathbf{v}_d(\mathbf{r})$, where $r = \sqrt{x^2 + y^2}$ is a distance from the center of rotation. Correspondingly, instead of Eq.(5) and (8), we define

$$L_z = \int_V \chi^T(0, 0, \Omega, r) r^2 d^3x \cdot \Omega, \quad (28)$$

and

$$I_z(\Omega) = I_z^{cl} - \lim_{q \rightarrow 0} \int_V \left[\frac{q^2}{q_\mu q_\nu} \hat{\chi}_{\mu\nu}(q, 0, \Omega, r) \right] r^2 d^3x. \quad (29)$$

The position-dependent rotational velocity is defined as

$$\Omega_0(\mathbf{r}) = \left(1 - \frac{1}{\rho} \lim_{q \rightarrow 0} \left[\frac{q^2}{q_\mu q_\nu} \hat{\chi}_{\mu\nu}(q, 0, \Omega, r) \right] \right) \Omega. \quad (30)$$

We extend the mechanical superfluid density $\hat{\rho}_s(T)$ in Eq.(26) so that it has Ω and r dependence and satisfies $\hat{\rho}_s(T, \Omega) = \int \hat{\rho}_s(T, \Omega, r) 2\pi r dr dz$ as

$$\hat{\rho}_s(T, \Omega, r) = \lim_{q \rightarrow 0} \left[\frac{q^2}{q_\mu q_\nu} \hat{\chi}_{\mu\nu}(q, 0, \Omega, r) \right]. \quad (31)$$

Let us consider the first approximation of the above quantities. We begin with

$$\langle J_\mu(x, t) \rangle = \langle G | S^\dagger \hat{J}_\mu(x, t) S | G \rangle, \quad (32)$$

where $S = T \exp \left[-i \int_{-\infty}^t dt' \hat{H}_{ex}(\mathbf{r}, t') \right]$. Using $H_{ex}(\mathbf{r}) = -v_d^\mu(\mathbf{r}) J_\mu(\mathbf{r})$, the analytical continuation $t \rightarrow \tau = it$ is performed in the higher-order expansion terms

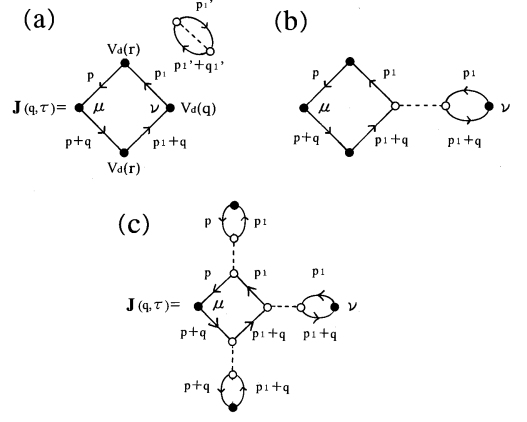


FIG. 4: (a) The third-order Feynman diagram of the current-current response tensor accompanied by the bubble excitation. (The definition of symbols is same as in Fig.3.) The exchange of particle at one vertex yields (b). Similar exchanges at the other vertices yield (c).

in the right-hand side of Eq.(32) [17]. As the simplest nonlinear susceptibility for J_μ , we consider the third-order term $\chi_{\mu, \nu \sigma \tau}^{(3)} v_d^\nu v_d^\sigma v_d^\tau$ with respect to H_{ex} and extract a correction term to the linear susceptibility $\chi_{\mu\nu}^{(3)}(v_d) \mathbf{v}_d$ from $\chi_{\mu, \nu \sigma \tau}^{(3)} v_d^\nu v_d^\sigma v_d^\tau$. $\chi_{\mu\nu}^{(3)}(v_d)$ is illustrated as a square in Fig.4(a), in which we choose only one vertex out of three vertices for the coupling to $\mathbf{v}_d(\mathbf{q})$ and make the others couple to the coarse-grained external field $\mathbf{v}_d(\mathbf{r})$. The lowest-order dynamic response of $I_z(\Omega)$ is obtained through $\chi_{\mu\nu}^{(3)}(v_d)$. (From now, we express $\chi_{\mu\nu}^{(3)}(v_d)$ by $\chi_{\mu\nu}^{(3)}(q, i\omega)$.)

Comparing Fig.3(a) and 4(a), we find that p in the lower bubble of Fig.3(a) splits into p and p_1 in Fig.4(a). We obtain a formula corresponding to the square in Fig.4(a)

$$\begin{aligned} \chi_{\mu\nu}^{(3)}(q, i\omega) &= \beta n_0 |\mathbf{v}_d(\mathbf{r})|^2 \frac{1}{\beta^2} \sum_{n, m} \frac{1}{V^2} \sum_{p, p_1} \left(p + \frac{q}{2} \right)_\mu \\ &\times \left(p_1 + \frac{q}{2} \right)_\nu \left(\frac{p + p_1}{2} \right) \cdot \left(\frac{p + p_1}{2} + q \right) \\ &\times G(i\omega_n + i\omega, p + q) G(i\omega_n, p) \\ &\times G(i\omega_m + i\omega, p_1 + q) G(i\omega_m, p_1), \end{aligned} \quad (33)$$

where $[(p + p_1)/2] \cdot [(p + p_1)/2 + q]$ comes from the coupling to the upper and lower $\mathbf{v}_d(\mathbf{r})$ in Fig.4(a). In general, a loop with four vertices has three inner frequencies ω_n, ω_m , and ω_l . For the susceptibility like Fig.4(a), however, the q, ω in $\chi_{\mu\nu}(q, i\omega)$ enters at one of the four vertices and leaves at another, thus leaving only two frequencies ω_n, ω_m as internal ones in Eq.(33). The remaining \hat{H}_{ex} in $\int_0^\beta d\tau \hat{H}_{ex}$, corresponding to ω_l , appears as $\beta \hat{H}_{ex} (= \beta n_0 |\mathbf{v}_d(\mathbf{r})|^2)$, since the macroscopic $\hat{v}_d(r)$ in \hat{H}_{ex} slowly varies with τ .

(a) With decreasing temperature, the coherent wave functions gradually grow, and therefore the particle interchange owing to Bose statistics frequently occurs in $\chi_{\mu\nu}^{(3)}$. By applying Eq.(13)-like formula for the product of four currents, we obtain a perturbation expansion of $\chi_{\mu\nu}^{(3)}$ with respect to the repulsive interaction H_I . Figure.4(a) illustrates the square surrounded by a bubble in $|G\rangle$ (an analogue of Fig.3(a)). The particle interchange at one of three vertices yields Fig.4(b). Fig.4(c) shows a horizontal and vertical extension of bubble chains.

(b) With decreasing temperature, particles stationary to a container get to play a dominant role. Comparing Fig.3(c) and Fig.4(b), we apply the argument above Eq.(15) to Eq.(33), knowing that $p = 0$ and $p = -q$ plays a dominant role in the sum over p . In the sum over p_1 as well, the dominant process comes from $p_1 = 0$ and $p_1 = -q$. At first sight, there seems to be four combinations in (p, p_1) . Owing to $(\mathbf{p} + \mathbf{p}_1)/2$ and $(\mathbf{p} + \mathbf{p}_1)/2 + \mathbf{q}$ in Eq.(33), however, only $(p, p_1) = (0, -q)$ and $(-q, 0)$ are possible. In Fig.4(a), the coupling to $v_d(q)$ is possible on the upper or lower vertex as well. Although this case has a different expression of $\chi_{\mu\nu}^{(3)}(q, i\omega)$ from Eq.(33), the particle interchange and the dominance of $p = 0$ or $p = -q$ particles derive the same formula from its $\chi_{\mu\nu}^{(3)}(q, i\omega)$, giving the final result the symmetry factor 2. Hence, one obtains the term representing the balance between the longitudinal and transverse susceptibility for the square in Fig.4(a)

$$\hat{\chi}_{\mu\nu}^{(3)}(q, 0, \Omega, r) = -q_\mu q_\nu \frac{1}{V^2} \left(\frac{q^2}{4} \right) |F_\beta(q)|^2 (\Omega r)^2 \beta n_0(T). \quad (34)$$

The process from Fig.4(a) to (c) changes Eq.(34) as follows. Using Eq.(13)-like formula for the product of four currents, bubble chains in Fig.4(c) are extended to infinity. Among these terms, to derive the nonclassical $I_z(\Omega)$ in Eq.(29), we pick up only terms that give a factor proportional to $q_\mu q_\nu / q^2$ at $q \rightarrow 0$ limit because other terms vanish in the $q \rightarrow 0$ limit of Eq.(29). Hence,

$$\hat{\chi}_{\mu\nu}^{(3)}(q, 0, \Omega, r) = -\frac{q_\mu q_\nu}{2} \left(\frac{q^2}{2} \right) \frac{1}{V^2 n^2} \times \frac{|F_\beta(q)|^2}{[1 - UF_\beta(q)]^2} (\Omega r)^2 \beta n_0(T). \quad (35)$$

Similarly to Eq.(18), the instability occurs in Eq.(35) when the condition of Eq.(20) is satisfied, because the denominator in the right-hand side of Eq.(35) gives q^{-4} , and therefore the coefficient of $q_\mu q_\nu$ diverges as q^{-2} at $q = 0$. At $T = T_{on}$, the same procedure as that from Eq.(18) to (21) yields

$$\hat{\chi}_{\mu\nu}^{(3)}(q, 0, \Omega, r) = -\frac{1}{V^2} \left(\frac{2m}{U\beta_{on}} \right)^2 \beta_{on} \frac{1}{n^2} n_0(T_{on}) \times \tanh^2 \left(\frac{\beta_{on}[\mu(T_{on}) - \Sigma]}{2} \right) (\Omega r)^2 \frac{q_\mu q_\nu}{q^2}, \quad (36)$$

and with the aid of Eq.(20)

$$\hat{\chi}_{\mu\nu}^{(3)}(q, 0, \Omega, r) = -\frac{mn_0(T_{on})}{V^2} \left(\frac{m(\Omega r)^2}{k_B T_{on}} \right) \times \frac{1}{n^2} \frac{1}{\sinh^2(\beta_{on}[\mu(T_{on}) - \Sigma])} \frac{q_\mu q_\nu}{q^2}. \quad (37)$$

Using $\hat{\rho}_s(T) = mc(T)n_0(T)$ as in Eq.(23), we obtain

$$\hat{\chi}_{\mu\nu}^{(3)}(q, 0, \Omega, r) = -mn_0(T_{on}) \left(\frac{\hat{\rho}_s(T_{on})}{\rho} \right)^2 \left(\frac{m(\Omega r)^2}{k_B T_{on}} \right) \frac{q_\mu q_\nu}{q^2}. \quad (38)$$

Substituting Eqs.(23) and (38) to Eq.(30) and using $mn_0/\rho = c^{-1}(\hat{\rho}_s/\rho)$ from the definition of $\hat{\rho}_s$, we get at $T \leq T_{on}$

$$\mathbf{\Omega}_0(\mathbf{r}) = \left[1 - \frac{\hat{\rho}_s(T)}{\rho} + \frac{1}{c(T)} \left(\frac{\hat{\rho}_s(T)}{\rho} \right)^3 \frac{m(\Omega r)^2}{k_B T} \right] \mathbf{\Omega}. \quad (39)$$

Using Eq.(39), we obtain a velocity field $\mathbf{v}_0(\mathbf{r}) = \mathbf{\Omega}_0(\mathbf{r}) \times \mathbf{r}$, and a vorticity field

$$\text{rot} \mathbf{v}_0(\mathbf{r}) = 2\mathbf{\Omega} \left[1 - \frac{\hat{\rho}_s(T)}{\rho} + \frac{2}{c(T)} \left(\frac{\hat{\rho}_s(T)}{\rho} \right)^3 \frac{m(\Omega r)^2}{k_B T} \right] \mathbf{e}_z. \quad (40)$$

This form shows a little change from $\text{rot} \mathbf{v} = 2\mathbf{\Omega} \mathbf{e}_z$ to $\text{rot} \mathbf{v} = 0$, that is, from a normal fluid to a superfluid. These results are summarized in the mechanical superfluid density

$$\hat{\rho}_s(T, \Omega, r) = \hat{\rho}_s(T) \left[1 - \frac{1}{c(T)} \left(\frac{\hat{\rho}_s(T)}{\rho} \right)^2 \frac{m(\Omega r)^2}{k_B T} \right]. \quad (41)$$

In a liquid helium 4, $m/k_B \cong 2.13 \times 10^{-8} \text{ sec}^2/\text{cm}^2$. Hence, the Ω dependence of Eq.(41) is negligibly small.

When the container is rotated in the normal phase, a liquid makes the rigid-body rotation satisfying $\mathbf{v}_d(\mathbf{r}) = \mathbf{\Omega} \times \mathbf{r}$. In the superfluid phase, a quantum vortex appears and a liquid makes a peculiar rotation satisfying $\mathbf{v}(\mathbf{r}) = (\hbar l/m) \mathbf{e}_z \times \mathbf{r}/r^2$ (l is an integer) being independent of Ω . At $T_\lambda < T < T_{on}$, however, while a liquid follows the rotation of a container, a region around the center of rotation slightly reduces its rotational velocity. Hence, the velocity field in a container takes an intermediate form between the velocity near the center and at the boundary. One can call it a *differential rotation* [18].

(1) Near the boundary, $\mathbf{v}_d(\mathbf{r}) = \mathbf{\Omega} \times \mathbf{r}$ becomes a large external field, and more higher-order terms than $\chi^{(3)}$ will contribute to $I_z(\Omega)$. Presumably, this will suppress superfluidity, and $\mathbf{v}_0(\mathbf{r}) = \mathbf{\Omega}_0(\mathbf{r}) \times \mathbf{r}$ with Eq.(39) will approach $\mathbf{v}_d(\mathbf{r}) = \mathbf{\Omega} \times \mathbf{r}$ of the rigid-body rotation.

(2) When one increases the rotational velocity Ω of a container, one can expect a similar result. With increasing Ω , the region rotating more slowly than the container will shrink to the center of rotation, and therefore the

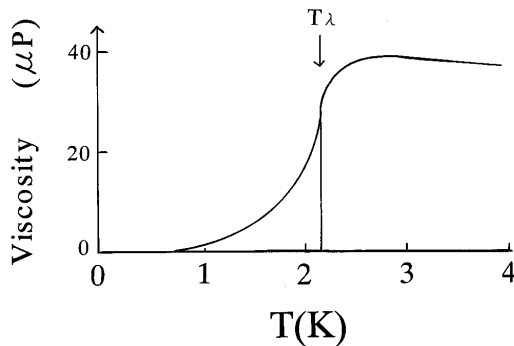


FIG. 5: The temperature dependence of the shear viscosity of a liquid helium 4. (The data at $T > T_\lambda$ is taken from Fig.3 of Ref.[19]. The data at $T < T_\lambda$ that strongly depends on the experimental method is written schematically.).

nonclassical I_z will approach the classical one as illustrated by a dotted line d in Fig.1.

(3) As $T \rightarrow T_\lambda$, the region near the center of rotation, which has a smaller vorticity, will enlarge toward the wall. (To describe such a growth and shrink, the effect of the wall must be taken into account as a boundary condition.)

(4) At $T < T_\lambda$, the nonclassical behavior discussed in this paper is masked by the quantum jump of L_z owing to the emergence of the quantum vortex. If the quantum vortex could be suppressed, one would see the hidden behavior of $L_z(\Omega)$, that is, Eq.(39) with $\hat{\rho}_s(T)/\rho = 1$.

VI. DISCUSSION

A. Shear viscosity at the vicinity of T_λ

In a classical liquid, with decreasing temperature, the shear viscosity gradually increases. The shear viscosity of a liquid is inversely proportional to the rate of a process in which a hole in a liquid propagates from one point to another over the energy barriers. With decreasing temperature, this rate decreases, thus increasing the viscosity. In a liquid helium 4, however, it reaches a maximum value at 2.8K, and begins to reduce its value, finally dropping at the λ point (2.17K). Figure.5 illustrates this temperature dependence taken from the data at $T > T_\lambda$ in [19]. In view of some precursory phenomena observed in a liquid helium 4, it is natural to explain it in terms of the thermal fluctuations giving rise to the short-lived wave function.

From the viewpoint of this paper, however, one must point out two other aspects of this phenomenon. (1) Under the strong influence of Bose statistics just above T_λ , the large but not yet macroscopic long-lived coher-

ent wave function must affect the response of the system. One must have a microscopic theory describing the influence of superfluidity on the coefficient of viscosity η , irrespective of whether the decrease of η is caused by the fluctuations or by the long-lived wave functions. For such a theory, (a) one must apply the linear-response theory not to the mechanical, but to the thermal perturbation [20]. The formulation of the latter perturbation includes more subtle points than that of the former one owing to the thermal dissipation. (b) The mechanism of shear viscosity in a liquid, which has similarities with the motion of dislocations in a solid, is considerably different from that of shear viscosity in a gas. Hence, the quasiparticle approximation, which is often used for the excitations in a liquid helium 4, is questionable for the shear viscosity in a liquid. The microscopic theory of the influence of superfluidity on η is a future problem.

(2) The viscosity appears in the Navier-Stokes equation as $\eta \Delta \mathbf{v}$, which has a form of $-\eta \cdot \text{rot}(\text{rot} \mathbf{v})$ in an incompressible fluid. The decrease of the viscosity comes from either the decrease of η or that of $\text{rot} \mathbf{v}$ [2]. The former is owing to the microscopic change of the system, whereas the latter arises from the macroscopic transformation of the velocity field $\mathbf{v}(\mathbf{r})$ in a container. At $T < T_\lambda$, the temperature dependence of the shear viscosity strongly depends on the experimental methods, such as (1) a Poiseuille flow method (a lower horizontal line at $T < T_\lambda$ in Fig.5), (2) an oscillating disc viscometer method (an upper curve at $T < T_\lambda$) and (3) a rotation viscometer method. Since the microscopic mechanism determining η is not sensitive to the types of the macroscopic measurements, this fact suggests that the shear viscosity at $T < T_\lambda$ is strongly dependent on the macroscopic change of $\text{rot} \mathbf{v}$ induced by the measurements. Above T_λ , however, since the coherent wave function has not yet grown to a macroscopic size, it is natural to attribute the decrease of viscosity at first to that of η . Just above T_λ , however, we have another possibility in $-\eta \cdot \text{rot}(\text{rot} \mathbf{v})$ that the emergence of the intermediate-sized coherent wave functions contributes to the decrease of $\text{rot} \mathbf{v}$, because they are irrotational. This means that the microscopic mechanism of a liquid affects not only the coefficient η , but also the macroscopic velocity field $\mathbf{v}(\mathbf{r})$. This is a peculiar case in fluid mechanics. In fluid mechanics, the velocity field $\mathbf{v}(\mathbf{r})$ is a solution of the equations of motion with given coefficients made of mechanical or thermodynamical constants of a liquid. In the system such as a liquid helium 4, one cannot clearly distinguish between the microscopic and macroscopic phenomena, and therefore, *this clear separation of coefficient and solution of the equation is not obvious* in contrast with a classical liquid. One must make a different approach that will examine the foundation of the two-fluid mechanics at the vicinity of T_λ .

B. Various manifestations of superfluidity

Superfluidity is a complex of phenomena, and therefore has some different manifestations, such as (1) persistent current without friction, (2) the Hess-Fairbank effect, (3) quantized circulation, (4) almost no friction on moving objects in the system below the critical velocity, (5) peculiar collective excitations and (6) the Josephson effect. The conventional thermodynamical definition of superfluid density $\rho_s(T)$ has been proved to be useful for describing various mechanical manifestations of superfluidity. The result of this paper implies that *the superfluid density in the mechanical phenomena does not always agree with the thermodynamical $\rho_s(T)$* , and that the interplay between Bose statistics and the repulsive interaction sometimes require us to define *the mechanical superfluid density* $\hat{\rho}_s(T)$. This $\hat{\rho}_s(T)$ may have some different definitions, each of which is specific to each manifestation of superfluidity, such as $\hat{\rho}_s(T)$ in Eq.(26) for the rotation. Hence, we must consider the existence or non-existence of $\hat{\rho}_s(T)$ in each manifestation on a case-by-case basis. Here we make a comment on three examples.

(A) The Meissner effect in the charged Bose system is a counterpart of the nonclassical rotational behavior in the neutral Bose system [8] [9]. (The enhanced diamagnetism above T_{BEC} appears as the precursory phenomenon owing to thermal fluctuations [21].) The phenomenon like the decrease of I_z , not owing to fluctuations but requiring a transformation extending to the whole system, occurs just above T_{BEC} in the Meissner effect as well: With decreasing temperature, the charged Bose gas with short-range repulsion begins to exclude the magnetic field prior to the BEC [22]. In contrast with the enhanced diamagnetism, the exclusion of the applied magnetic field just above T_{BEC} implies that the large but not yet macroscopic wave functions cause a change extending to the whole system. This means that Bose statistics is essential for the Meissner effect, but the existence of the macroscopic condensate is not the necessary condition. The same form of the mechanical superfluid density $\hat{\rho}_s(T)$ is useful for the Meissner effect as well.

(B) The nonclassical rotational behavior above T_λ will become more realistic in superfluidity of *small systems*. Recently, a helium 4 droplet consisting of about 10^4 helium 4 atoms is found to show a sign of superfluidity. The infrared rotational spectrum of small molecules attached to the helium 4 droplet, such as oxygen carbon sulfide, shows a signal indicating a significant change of its moment of inertia around a molecular axis at $T < T_\lambda$, which suggests a transition occurring in the surrounding helium 4 environment [23]. Although the experimental condition, such as the temperature or the rotational velocity, cannot be freely controlled until now as in the bulk helium 4, it will open a new probability of superfluidity of small systems. If the same experiment as in Sec.4 could be made for a liquid helium 4 droplet, one would see a larger role of the intermediate-sized coherent wave function $\hat{\rho}_s(T_1)/\rho$ in the rotational properties [6]. When the

number of atoms in a droplet is too small, however, the λ transition will become obscure. Hence, there may be an optimum size of the system for detecting the nonclassical rotational behavior just above T_λ .

(C) Solid helium 4 has been termed a quantum crystal. Recently, an abrupt drop in the moment of inertia was found in the torsional oscillation measurements on solid helium 4 confined in a porous media [24] and on a bulk solid helium 4 [25]. This discovery leads us to reconsider the definition of superfluidity and that of solids [26]. The fundamental feature of crystals is their periodicity in density; that is, diagonal long-range order (DLRO). One has to face a serious question whether crystals remain stable while showing superfluidity that violates their periodicity. Phenomenologically, this discovery shares the following point with the subject of this paper: The non-classical decrease of the moment of inertia occurs even in the system in which the existence of the macroscopic Bose condensate is not expected. There is, however, the following difference. In a normal liquid helium 4 at the vicinity of T_λ , helium 4 atoms actually exist, and the size of their coherent wave function with zero momentum is a subject of the problem, whereas in a solid helium 4, the existence of a hypothetical moving boson, a zero-point vacancy, has not been firmly established, although it is normally assumed to exist. There are a number of problems to be clarified in a solid helium 4.

APPENDIX A: COMPARISON TO THE THERMAL FLUCTUATION

Compared with the thermal-fluctuation theories, the formalism in Sec.3 has the following differences. (1) In the fluctuation theory of a quantity x in question, the correlation function of deviations $x - \bar{x}$ from a mean value \bar{x} gives the susceptibility, an average of which is taken with the Gauss distribution. Owing to the flatness of the minimum of the thermodynamic potential near T_c , the susceptibility has $(1 - T/T_c)$ dependence. (Alternatively, the introduction of Green's functions representing thermal fluctuations leads to the similar $(1 - T/T_c)$ dependence.) On the other hand, the susceptibility in Sec.3 is given as the correlation function of total quantities x as in Eq.(9). Its average is taken with the Bose-Einstein distribution. Hence, the result has no $(1 - T/T_c)$ dependence. (2) Since thermal fluctuation is essentially a local phenomenon, one notes its influence already in the low-order terms of the perturbation expansion in which only a few particles participate. On the other hand, the change of the moment of inertia I_z requires a transformation extending to the whole liquid. Hence, the higher-order terms in which many particles participate plays a significant role. Only after the perturbation expansion is summed up to the infinite order as in Eq.(18), one notices the change of I_z at a temperature in which Eq.(20) is satisfied.

(3) Thermal fluctuations gradually increase as $T \rightarrow T_c$,

finally diverging at T_c . For the change of the moment of inertia, however, no physical relevant quantity diverges

at T_c , and I_z smoothly agrees with the conventional value of $I_z^{cl}(1 - \rho_s/\rho)$ as in Eq.(26).

-
- [1] The variational theory at the vicinity of T_λ , which assumes the expandibility of the thermodynamic potential in powers of the small order parameter, belongs to this category.
 - [2] F.London *Superfluid*, (John Wiley and Sons, New York, 1954) Vol.2, 141.
 - [3] G.B.Hess and W.M.Fairbank, *Phys.Rev.***19**, 216(1967)
 - [4] As a text, R.J.Donnelly, *Quantized Vortices in Helium 2*, (Cambridge, 1991)
 - [5] R.E.Packard and T.M.Sanders, *Phys.Rev.***6**, 799(1972)
 - [6] In the equation of states $N/V = g_{3/2}(e^{\beta\mu}) + V^{-1}e^{\beta\mu}/(1 - e^{\beta\mu})$ where $g_a(x) = \sum_n x^n/n^a$, $V^{-1}e^{\beta\mu}/(1 - e^{\beta\mu})$ has a finite value at $V \rightarrow \infty$ limit only when $e^{\beta\mu}/(1 - e^{\beta\mu})$ diverges. Hence, this limit decomposes all states into only two classes, the condensate and the whole of other states, and therefore each of other states loses its characteristics.
 - [7] F.Chevy, K.W.Madison and J.Daiibard, *Phys.Rev. Lett.***85**, 2223(2000).
 - [8] As a review, P.Nozières, in *Quantum Fluids* (ed by D.E.Brewer), 1 (North Holland, Amsterdam, 1966).
 - [9] As a review, G.Baym, in *Mathematical methods in Solid State and Superfluid Theory* (ed by R.C.Clark and G.H.Derrick), 121 (Oliver and Boyd, Edingburgh, 1969)
 - [10] Whatever complicated approximation is made for the susceptibility, this treatment enables us to derive the superfluid density from it.
 - [11] R.P.Feynman, in *Progress in Low Temp Phys.* **1**, (ed C.J.Gorter), 17 (North-Holland, Amsterdam, 1955).
 - [12] It is possible that more complex diagrams than the bubble in $|G >$ may participate in the particle exchange with the tensor $J_\mu J_\nu$ in Fig.3(a). Although it is difficult to estimate an infinite sum of these diagrams, it adds only a small correction to the whole feature of the phenomenon.
 - [13] In an attractive Bose gas ($U < 0$), the instability condition leading to a liquid state is recently found as $\mu(T) = -\sqrt{-Uk_B T}$ in S.Koh, *Phys.Rev.E*,**72**, 016104(2005). It is suggestive that, in a response to the external perturbation, a similar-looking instability condition $\mu(T) - \Sigma(U) = -\sqrt{Uk_B T}$ appears in a different context of the repulsive Bose system ($U > 0$).
 - [14] T.Matsubara, *Prog.Theo.Phys.***6**, 714 (1951).
 - [15] R.P.Feynman, *Phys.Rev.* **90**, 1116 (1953), *ibid* **91**, 1291 (1953).
 - [16] The total density ρ of a liquid helium 4 exhibits a slight change at the vicinity of T_λ (E.C.Kerr and R.D.Taylor, *Ann.Phys.* **26**, 292(1964)), but it does not affect the ratio $\hat{\rho}_s/\rho$.
 - [17] The analytic continuation of the real-time susceptibility to the imaginary-time one was originated by Abrikosov, Gorkov and Dzyaloshinskii. This procedure was extended to the higher-order susceptibility in the interaction representation by V.V.Slezov in *Fiz.Tverd.tela*,**5**, 2958(1963) [*Sov.Phys-Solid.State*,**5**, 2166(1963)]
 - [18] For the differential rotation in astrophysics, such as that of rotating stars or galaxies, the peripheral region does not follow the rigid-body rotation, because the driving force of rotation is given at the center. On the contrary, for the differential rotation of a superfluid in a bucket, the central region does not follow the rigid-body rotation.
 - [19] R.D.Taylor and J.G.Dash, *Phys.Rev.***106**, 398(1957)
 - [20] L.P.Kadanoff and P.C.Martin, *Ann.Phys.* **24**, 419(1963).
 - [21] For the electron superconductivity, J.P.Gollub, M.R.Beasley, R.S.Newbower and M.Tinkham, *Phys.Rev.Lett.* **22**, 1288(1969).
 - [22] S.Koh, *Phys.Rev.B.* **68**, 144502 (2003), *B.***73**, (E)029902 (2006).
 - [23] S.Grebenev, J.P.Toennies and A.F.Vilesov, *Science*.**279**,2083(1998).
 - [24] E.Kim and M.H.W.Chan, *Nature*. **427**, 225(2004).
 - [25] E.Kim and M.H.W.Chan, *Science*. **305**, 1941(2004).
 - [26] A.J.Leggett, *Phys.Rev. Lett.***25**,1543(1970).